

## High Performance Cúk Converter Considering Non-Linear Inductors for Photovoltaic System Applications

E. Shokati Asl\*, M. Shadnam Zarbil, M. Sabahi

Faculty of Electrical and Computer Engineering, University of Tabriz, Tabriz, Iran

### ABSTRACT

*The Cúk converter, which has voltage buck and boost ability, offers high flexibility as an interface device for solar panels. In addition, current ripple can be more reduced because of two input and output inductors at both sides. This paper presents a new application of current-variable inductors in a Cúk converter that reduces the size and capacity of storage elements. Because of two inductors in structure, implementation of these variable inductors is important; therefore, the proposed design leads to cost and size savings, increases the performance interval of tracker to gain solar energy at lower sunlight levels, and simplifies control strategy. To validate the effectiveness of this structure, the analytical analysis, simulation results using PSCAD/EMTDC software and experimental results are presented.*

**KEYWORDS:** Variable inductor, Photovoltaic, Obtaining maximum power, Impedance match, Cúk converter.

### 1. INTRODUCTION

In recent years, increasing environmental concerns has led to more attention to renewable energy, instead of fossil fuels [1, 2]. Hence, widespread works have been conducted on the interfaces of power electronics for renewable energy systems. In [3], various practiced methods in power electronic interfaces were presented to tap energy from hybrid renewable energy sources. Also, in this survey, the efficient storage system technology was investigated for hybrid wind solar power generation system. In [4], the special study was focused on dc converter. This investigation explored important characteristics of multiple-input converters (MIC) serving as a power electronic interface for renewable energy applications. The advantages of MICs were explained and feasible MIC topologies for renewable energy applications were discussed and classified into four different MIC families. Design considerations for extending MIC's voltage step-up ratio and achieving maximum power point tracking on all PV sources were presented as well. The

improvements in the semiconductor technology has led to paying more attention for solar or photovoltaic (PV) panels. PV systems are costly; therefore, several works have been performed to improve the efficiency of solar energy conversion [5]. Also, altered methods for maximum power point tracking (MPPT) have been presented in different weather situations. In [6], a method for maximum power point tracking (MPPT) control was described while searching for the optimal parameters corresponding to weather conditions at that time. In [7], a systematic approach suitable for modeling the behavior of a photovoltaic field operating in both uniform and mismatched conditions was shown. The presented approach was intended to evaluate the long-term energetic performances of photovoltaic fields on a daily, monthly, or yearly basis where a fast computation process had to be achieved. There are many factors that can reduce the output power of a PV: partial shading [8, 9] caused by clouds, towers, and trees [10]. In [8], an exhaustive study of the available interconnections among the modules of a shaded photovoltaic field was done and, as a result, a clear relationship was presented between the interconnections of the PV modules and their power output through empirical connection laws. In [9], a

Received: 10 May 2015

Revised: 06 Sep. 2015

Accepted: 20 Sep. 2015

\*Corresponding author:

E. Shokati Asl (E-mail: e.shokati92@ms.tabrizu.ac.ir)

© 2015 University of Mohaghegh Ardabili

fixed interconnection scheme was presented for PV arrays that enhanced the PV power under different shading conditions. The presented scheme facilitated the effect distribution of shading over the entire array, thereby reducing the mismatch losses caused by partial shading. In most papers, modeling of partial shading has been done on PV modules to design a suitable controller and achieve the maximum output power [11, 12]. During the operation of a DC-DC converter, it is possible for the converter to work in two continuous and discontinuous modes to get maximum power. Thus, the implementation of two different controllers is obtained to obtain maximum power in any condition [13]. These two controllers not only cause complexity in circuit, but also lead to the cost increment of additional current sensor for DCM operation. In [14], a variable inductor was used to preserve continuous conduction in partial shading to obtain maximum power from the controller. Nevertheless, buck converter only can reduce voltage with no step-up capability; therefore, it cannot scan the whole PV area and MPPT is sometimes lost [15]. Also, because of the variable inductor in the buck converter, overall current ripple becomes high, which is not suitable enough for PV systems.

In this paper, the Cúk converter with variable inductors for photovoltaic system is proposed. This converter which has the voltage buck and boost ability can scan the whole PV voltage and current characteristic curve to obtain the point of maximum power. Moreover, it has a lower current ripple than the buck converter. The proposed structure reduces the cost of inductors, decreases number of controllers from two to one at low solar irradiations, and increases performance intervals of the tracker to get solar energy in partial shading conditions. In Section 2, the maximum power extracting method by the Cúk converter with variable inductor is discussed. In Section 3, the minimum required inductance, which guarantees continuous conduction mode (CCM), is calculated. In Section 4, the structure of an inductor with variable inductance is analyzed. In Section 5, the proper values of capacitors for the Cúk converter are achieved. In Section 6, simulation and experimental results are

presented to prove the proposed circuit. In Section 7, conclusions are presented.

## 2. MPPT METHOD

To extract the PV maximum power, several methods, e.g. P&O or ICM, are usually used. In the ICM method, based on maximum power transfer principle, output resistance of PV panel must be equal to the load resistance. According to Fig. 1, it can be done by the linearization of I-V characteristics of a PV panel in its knee area; hence,  $r$ , the equivalent resistance at maximum power point, can be specified by Eq. (1).

$$-r = -\frac{\Delta V}{\Delta I} = R_{LR} = \frac{V_p}{I_p} \quad (1)$$

where  $R_{LR}$  is the input equivalent resistance of the Cúk converter to get to MPPT,  $V_p$  and  $I_p$  are the PV voltage and current in MPP, respectively. The voltage gain in CCM is as follows [16]:

$$\frac{V_o}{V_p} = \frac{D}{1-D} \quad (2)$$

where  $V_o$  and  $D$  are the output voltage and duty-cycle, respectively. Assuming the efficiency of 100%, relation of output current and input current is calculated as:

$$\frac{I_o}{I_p} = \frac{1-D}{D} \quad (3)$$

where  $I_p$  is the mean input current in the Cúk converter and  $I_o$  is the mean output current of the Cúk converter. Equivalent resistance is obtained by replacing Eqs. (2) - (3) in Eq. (1) as follows:

$$R_{LR} = \frac{V_p}{I_p} = \frac{\frac{(1-D)V_o}{D}}{\frac{D}{(1-D)}I_o} = \frac{(1-D)^2}{D^2} R_L \quad (4)$$

where,  $R_L$  represents the output load resistance of the converter. Eq. (2) is true only during CCM mode operation of the Cúk converter. The variety of PV panel conditions, e.g. solar irradiation or temperature, can be easily compensated for by duty-cycle proper adjusting via controller unit to achieve MPP in any environments. In discontinuous current mode, DCM, Eq. (2) is not satisfied and stable operation of the converter becomes more complex.

In addition, in discontinuous conduction mode, DCM, power is a function of dead time; so, a different MPPT strategy is required.

### 3. MINIMUM INDUCTANCE FOR CCM

Minimum inductances in a Cúk converter that preserve the CCM are as follows [16]:

$$L_{1,\min} = \frac{(1-D)^2}{2Df_s} R_L \quad (5)$$

$$L_{2,\min} = \frac{(1-D)}{2f_s} R_L \quad (6)$$

where  $f_s$  is the switching frequency. Using Eq. (3), the minimum value of inductances,  $L_{1,\min}$  and  $L_{2,\min}$ , can be obtained as follows:

$$L_{1,\min} = \frac{(1-D)^2 V_o}{2Df_s I_o} = \frac{(1-D)V_P}{2f_s I_o} \quad (7)$$

$$L_{2,\min} = \frac{(1-D)V_o}{2f_s I_o} = \frac{DV_P}{2f_s I_o} \quad (8)$$

PV voltage is about constant at most solar irradiation levels [17]; therefore, the minimum inductances is mainly a function of  $D$ , output current,  $I_o$ , and switching frequency.

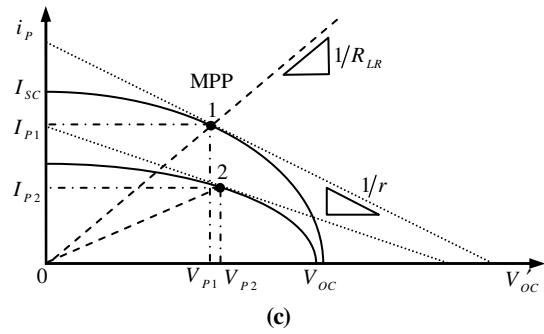
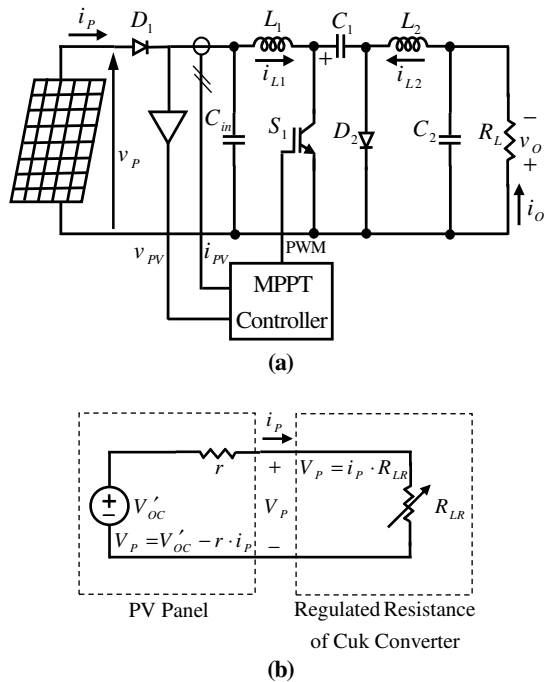
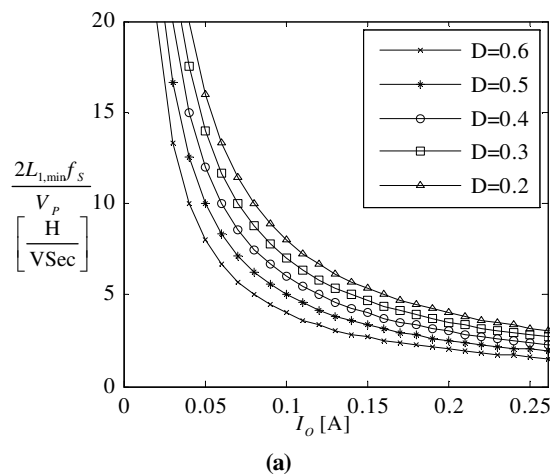
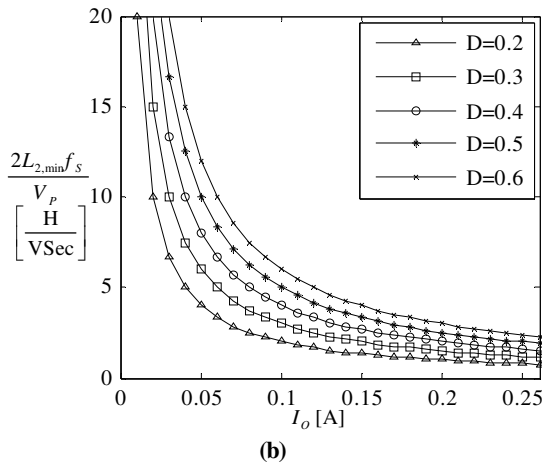


Fig. 1. Maximum PV power obtaining method; (a) MPPT test using the Cúk converter; (b) Equivalent Thevenin circuit; (c) MPPT according to impedance match.

Figure 2 shows the characteristic of  $L_{1,\min}$  and  $L_{2,\min}$  based on  $I_o$  for different  $D$  values. According to Fig. 2.a and Fig. 2.b,  $L_{1,\min}$  and  $L_{2,\min}$ , decreasing with the increase of  $D$ , i.e. to stay on CCM with small duty cycles and higher values of  $L_{1,\min}$  and  $L_{2,\min}$ , are required. Another basic point is that  $L_{1,\min}$  is equal to  $L_{2,\min}$  for  $D = 0.5$  and, to stay on CCM for  $D > 0.5$ , the value of  $L_{2,\min}$  is greater than  $L_{1,\min}$ ; therefore, by choosing two  $L_1$  and  $L_2$  with the greater value than  $L_{2,\min}$ , CCM is covered. For  $D < 0.5$ ,  $L_{2,\min}$  is smaller than  $L_{1,\min}$ ; i.e. by choosing two  $L_1$  and  $L_2$  inductors with the values of greater than the  $L_{1,\min}$ , CCM is obtained definitely.





**Fig. 2.** Characteristic of the minimum inductor to keep CCM based on the mean output current and different duty cycles; (a) first minimum inductor; (b) second minimum inductor.

**Table 1.** Comparison of the proposed Cúk converter with the conventional Cúk converter

	Proposed Cúk converter	Conventional Cúk converter
Need for dual controller	No	Yes
Weight	Low	High
Volume	Low	High
Cost	Low	High

According to Fig. 2, increasing  $I_o$ , that is related to small output resistance or increase of solar irradiation, causes the minimum inductor values to decrease. Also, decreasing  $I_o$ , that is related to the big output resistance or decrease of solar irradiation, causes the minimum inductor values to increase in order to preserve CCM. Table 1 shows the comparison between the proposed and conventional Cúk converters. According to this comparison, the proposed Cúk converter is better than the conventional Cúk converter for photovoltaic applications.

#### 4. INDUCTOR WITH VARIABLE INDUCTANCE

The values of inductors decrease to maintain CCM when solar irradiation increases. On the other hand, in small loads, their values increase and a variable inductor with this specification would have smaller size. To make a saturable inductor, a smaller size core, without air-gap or with a narrow air-gap, can be used practically. There are also other methods to construct variable inductors, e.g. using the powdered metal core [18, 19].

Figure 3 shows the important role of a variable inductor for stable performance of the Cúk converter.

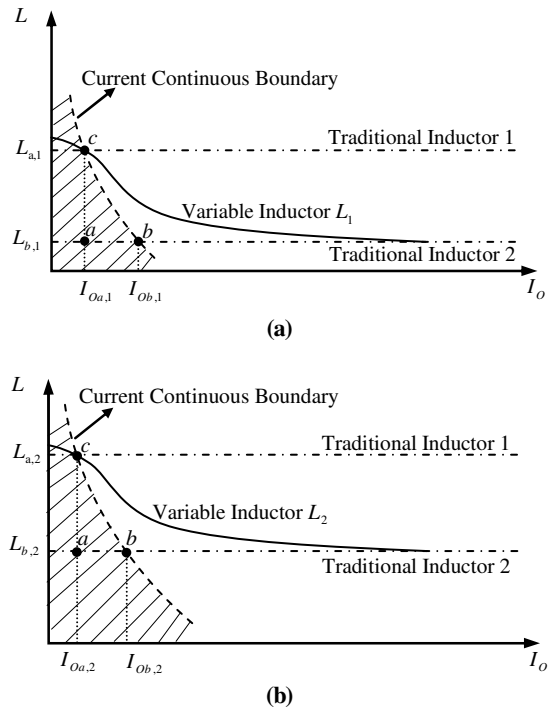


**Fig. 3.** Comparison of CCM condition in the Cúk converter with a variable inductor; (a) first variable inductor (b) second variable inductor.

Figure 3.a shows that the continuous conduction happens only by an inductance with values of higher than the hatched lines and lower limit of load current at low solar irradiation,  $I_{0a,1}$ , is proportional with inductor  $L_{a,1}$  and high current values,  $I_{0b,1}$ , is almost proportional to  $L_{b,1}$ . Fig. 3.b shows that lower limit of load current at low solar irradiation,  $I_{0a,2}$ , is almost proportional to  $L_{a,2}$  and high current values,  $I_{0b,2}$ , are almost proportional to  $L_{b,2}$ . Increased inductance in lower solar irradiation causes CCM maintenance; i.e. the control strategy of MPPT controller is expanded into lower solar irradiation levels. In other words, it keeps the same control strategy in the partial shading conditions. Characteristic of a linear time invariant inductor is as follows:

$$\phi(t) = Li(t) \quad (9)$$

Where,  $L$  is a constant and independent from  $t$  and  $i$ .

$$v(t) = L \frac{di}{dt} \quad (10)$$

In this paper, a variable inductor is used; therefore, the relationship between flux and inductance can be written as:

$$\phi = L(i)i \quad (11)$$

$$v(t) = \frac{d\phi}{dt} = L \frac{di}{dt} + i \frac{dL}{dt} = (L + i \frac{dL}{di}) \frac{di}{dt} = L_{eff} \frac{di}{dt} \quad (12)$$

In Eq. (12),  $L_{eff}$  can be obtained from  $L-i$  characteristic of the variable inductor.

### 5. CAPACITOR VALUES

Suitable design of element values leads to construction cost savings; therefore, designing the capacitor value is important. In the Cúk converter,  $C_1$  has an important role and energy transfer depends on it. The voltage ripple of  $C_1$  can be approximately determined according to its voltage when  $S_1$  is switched off. Under these conditions,  $i_{L1}$  and  $i_{C1}$  are the same. Assuming a superficial constant  $L_1$  current,  $I_{L1}$ , Eq. (13) is obtained as follows:

$$\Delta v_{C1} \approx \frac{1}{C_1} \int_{DT}^T I_{L1} dt = \frac{I_{L1}}{C_1} (1-D)T \quad (13)$$

Using Eqs. (2) and 3, Eq. (13) can be rewritten as:

$$\Delta v_{C1} \approx \frac{V_P}{R_L C_1 f_s} \left( \frac{D^2}{1-D} \right) \approx \frac{V_O D}{R_L C_1 f_s} \quad (14)$$

On the other hand, output elements,  $L_2$ ,  $C_2$ , and  $R_L$  have the same performance as in the buck converter. Therefore, ripple of the output voltage is achieved similarly as follows [16]:

$$\frac{\Delta V_O}{V_O} = \frac{(1-D)}{8L_2 C_2 f_s^2} \quad (15)$$

To specify  $C_1$  and  $C_2$ , Eqs. (14) and (15) can be used to obtain Eqs. (16) and (17), respectively:

$$C_1 = V_O D / (R_L f_s (\Delta v_{C1})) \quad (16)$$

$$C_2 = \frac{(1-D)}{8L_2 f_s^2 (\Delta V_O / V_O)} \quad (17)$$

### 6. SIMULATION AND EXPERIMENTAL RESULTS

To prove the discussed theories in the previous sections, the simulation and experimental results are presented. For the simulations and experimental setup, a 20W PV module was chosen. The electrical parameters of this module are tabulated in Table 2. The specifications of elements in the simulation is

shown in Table 3. Specifications of the experimental setup elements are presented in Table 4 and Fig. 4 demonstrates the experimental setup of the proposed structure.

**Table 2.** Electrical parameters of PV

Maximum power ( $P_{max}$ )	20 W
Voltage at MPP ( $V_{mpp}$ )	17.5 V
Current at MPP ( $I_{mpp}$ )	1.16 A
Open circuit voltage ( $V_{OC}$ )	21.01 V

**Table 3.** Selected values in simulation and experimental setup

$C_1 = C_{in}$	470µF
$C_2$	220µF
$r_{Switch-on}$	0.1Ω
$r_{Diode-on}$	0.1Ω
$R_L$	100Ω
$f_s$	20 kHz

**Table 4.** Values and specification of elements.

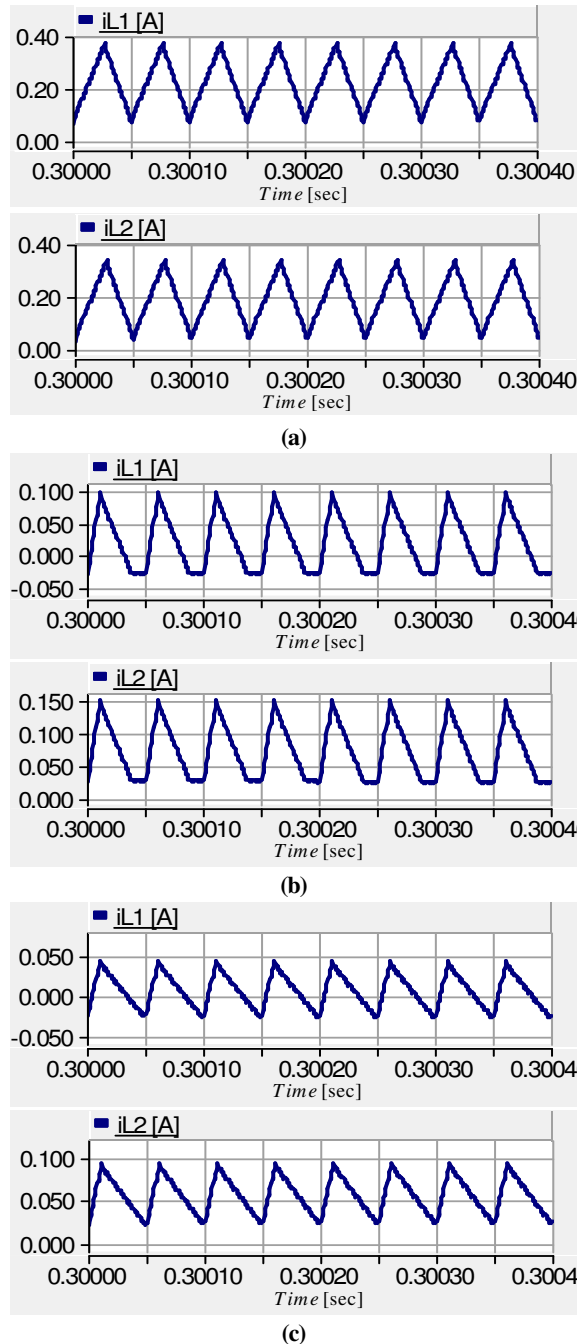
$C_1 = C_{in}$	470µF, 63V
$C_2$	220µF, 100V
Switch	IRF540N
Diode	MUR1560G
$R_L$	100Ω

#### 6.1. Simulation results

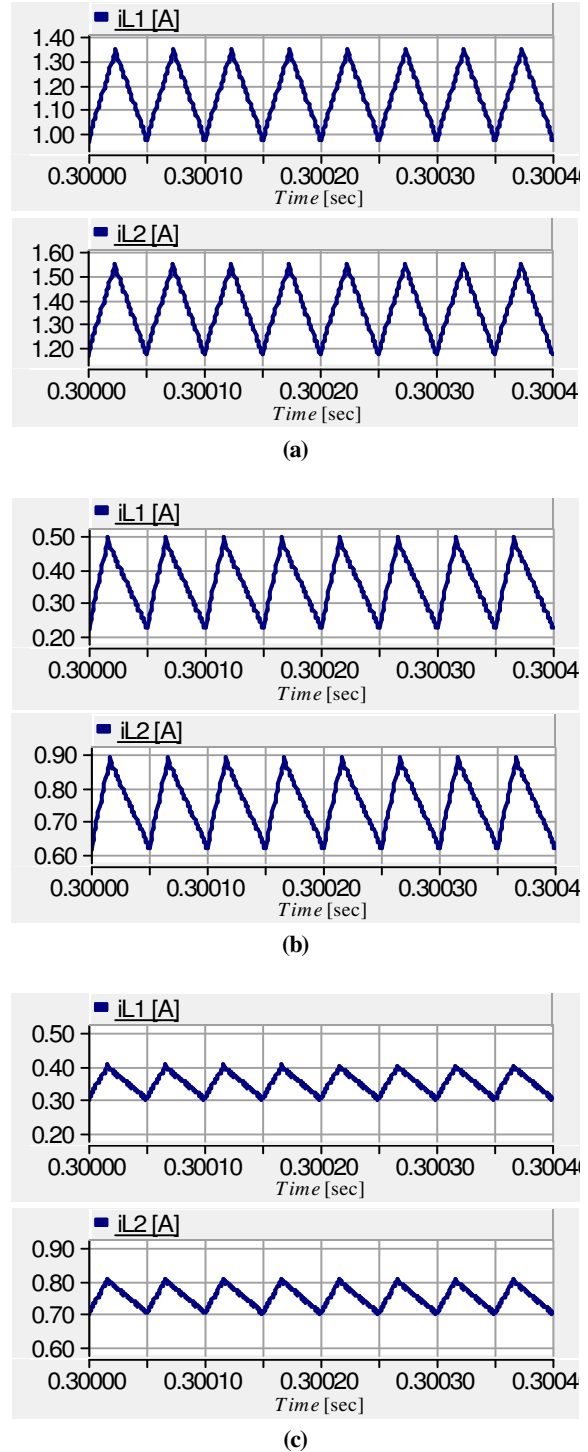
The simulation was conducted using PSCAD/EMTDC software. The resistance of inductors and ESR of capacitors were considered in the simulation. Figure 4.a shows  $i_{L1}$  and  $i_{L2}$  when  $L_1=L_2=1.5$  mH at high solar irradiation ( $G=250$  W/m<sup>2</sup>), in which  $i_{L1}$  and  $i_{L2}$  were in CCM. Figure 4.b presents the simulation results for  $i_{L1}$  and  $i_{L2}$  with the same inductor values at low solar irradiation ( $G=50$  W/m<sup>2</sup>). In this case,  $i_{L1}$  and  $i_{L2}$  were in DCM. Fig. 4.c shows  $i_{L1}$  and  $i_{L2}$  using variable inductors at low solar irradiation and CCM operation was achieved; hence, maximum power can be provided by a single controller unit and strategy. On the other hand, current ripple was decreased intensively because of the increased inductance of the variable inductor at low solar irradiation.

Figure 5.a shows the simulation results for the higher load conditions including  $i_{L1}$  and  $i_{L2}$  when  $L_1=L_2=1$  mH at high solar irradiation ( $G=900$  W/m<sup>2</sup>). In this case, CCM was acquired. Figure 5.b presents the simulation results for  $i_{L1}$  and  $i_{L2}$  with the

same inductor values, but at low solar irradiation ( $G=300 \text{ W/m}^2$ ), in which CCM was still obtained. Figure 5.c shows the simulation results for  $i_{L1}$  and  $i_{L2}$  using the variable inductors at low solar irradiation which caused low current ripple at low solar irradiation.



**Fig. 4.** Simulation results for currents of  $L_1$  and  $L_2$ ; (a) Invariable inductors'  $L_1$  and  $L_2$  currents at high solar irradiation ( $G=250 \text{ W/m}^2$ ) for  $L_1=L_2=1.5 \text{ mH}$ ; (b) Invariable inductors'  $L_1$  and  $L_2$  currents at low solar irradiation ( $G=50 \text{ W/m}^2$ ) for  $L_1=L_2=1.5 \text{ mH}$ ; (c) Variable inductors'  $L_1$  and  $L_2$  currents at low solar irradiation ( $G=50 \text{ W/m}^2$ ).



**Fig. 5.** Simulation results for the currents of  $L_1$  and  $L_2$ ; (a) Invariable inductors'  $L_1$  and  $L_2$  currents at high solar irradiation ( $G=900 \text{ W/m}^2$ ) for  $L_1=L_2=1 \text{ mH}$ ; (b) Invariable inductors'  $L_1$  and  $L_2$  currents at low solar irradiation ( $G=300 \text{ W/m}^2$ ) for  $L_1=L_2=1 \text{ mH}$ ; (c) Variable inductors'  $L_1$  and  $L_2$  currents at low solar irradiation ( $G=300 \text{ W/m}^2$ ).

## 6.2. Experimental results

Figure 6 shows the power circuit and MPPT controller. Figure 7 shows the experimental results

for currents of  $L_1$  and  $L_2$  at different solar irradiations. Figure 7.a is the experimental result for  $i_{L1}$  and  $i_{L2}$  when  $L_1=L_2=1.5$  mH for high luminous intensity. In this figure, inductors' current was in CCM. Figure 7.b presents the experimental results for  $i_{L1}$  and  $i_{L2}$  with the same inductor values, but at low solar irradiation. In this figure, inductors' current was in DCM. Figure 7.c shows the experimental results when using variable inductors at low solar irradiation and inductors' current was in CCM; hence, the performance interval of the MPP tracker was increased to get solar energy at lower solar irradiation. Also, the control strategy of MPP controller was expanded to low solar irradiation. It is worth mentioning that values for inductors  $L_1$  and  $L_2$  were chosen equal, because at high solar irradiation, to obtain maximum power,  $D$  was almost 0.5; therefore, values of  $L_{1,min}$  and  $L_{2,min}$  were the same. During low solar irradiation,  $D$  was 0.5 to get maximum power. So, the value of  $L_{2,min}$  was smaller than  $L_{1,min}$ . It means that, by choosing similar variable inductors and with the values of greater than  $L_{1,min}$ , CCM was ensured.

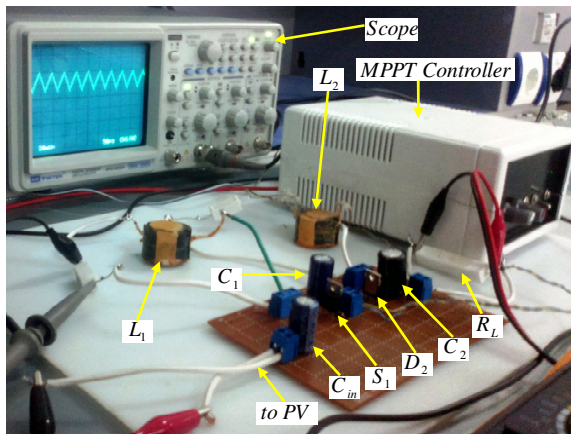
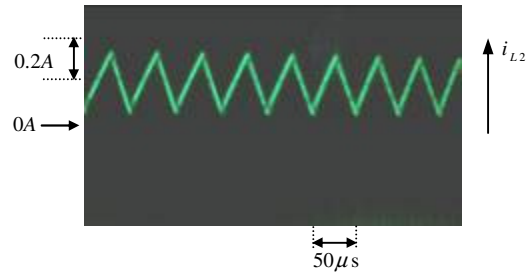
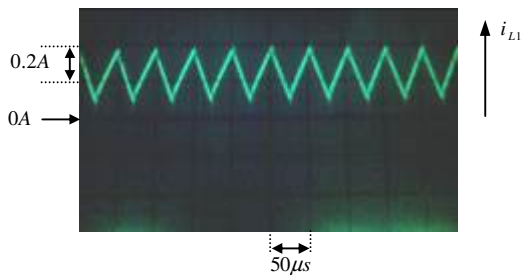
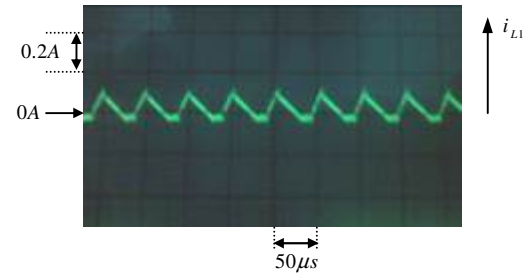


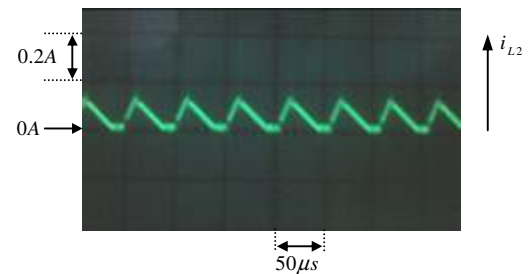
Fig. 6. Experimental circuit of the proposed structure.



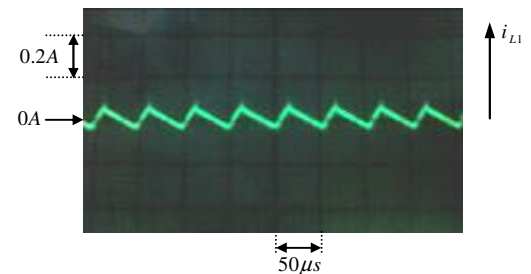
(a)



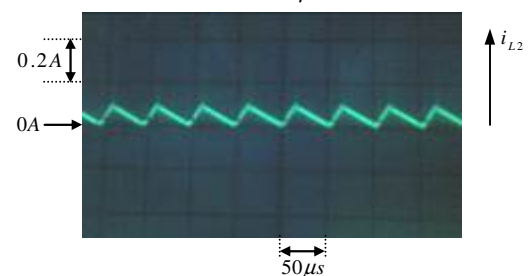
(b)



(c)



(a)



(b)

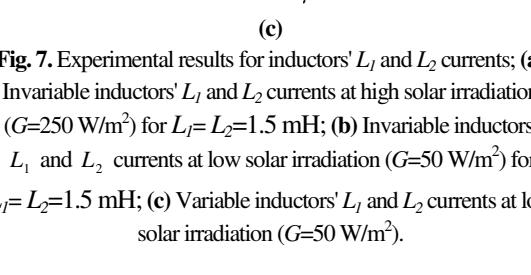


Fig. 7. Experimental results for inductors'  $L_1$  and  $L_2$  currents; (a) Invariable inductors'  $L_1$  and  $L_2$  currents at high solar irradiation ( $G=250$  W/m<sup>2</sup>) for  $L_1=L_2=1.5$  mH; (b) Invariable inductors'  $L_1$  and  $L_2$  currents at low solar irradiation ( $G=50$  W/m<sup>2</sup>) for  $L_1=L_2=1.5$  mH; (c) Variable inductors'  $L_1$  and  $L_2$  currents at low solar irradiation ( $G=50$  W/m<sup>2</sup>).

## 7. CONCLUSIONS

In this paper, a high performance Cúk converter was presented using nonlinear inductors for photovoltaic system applications. The main features achieved by the variable inductors, can be listed as follows:

- Simple control strategy,
- Low cost MPPT controller,
- Scanning capability of the whole I-V plane characteristic of PV panel, even in different weather conditions, like partial shading,
- Lower size and cost of inductors,
- Lower current ripples at low current levels.

Using the structure of the proposed discontinuous conduction mode, MPPT in different weather conditions was achieved; this ability cannot be found in the traditional buck converter. In addition, because of two input and output inductors, current ripple in the Cúk converter was much less than that of the buck converter. Considering the variable inductor characteristic, it is clear that, by current increment, its inductance decreased. This ability had different advantages, e.g. smaller inductor size and stability of control method in the partial shadings. Calculations of the minimum inductor value to keep CCM and design the Cúk's capacitors were conducted in a suitable way that led to cost saving. Conformity between theoretical results and simulation-experimental ones proved the effectiveness of the proposed structure.

## REFERENCES

- [1] M. Marinelli, P. Maule, A. Hahmann, O. Gehrke, P. Norgard and N. Cutululis, "Wind and photovoltaic large-scale regional models for hourly production evaluation," *IEEE Transactions on Sustainable Energy*, vol. 6, no. 3, pp. 916-923, 2015.
- [2] A. K. Abdelsalam, A. M. Massoud, S. Ahmed and P. N. Enjeti, "High-performance adaptive perturb and observe MPPT technique for photovoltaic-based microgrids," *IEEE Transactions on Power Electronics*, vol. 26, no. 4, pp. 1010-1021, 2011.
- [3] M. Manojkumar, K. Porkumaran and C. Kathirvel, "Power electronics interface for hybrid renewable energy system," *Proceeding of the International Conference on Green Computing Communication and Electrical Engineering*, pp. 1-9, 2014.
- [4] R. Zhao, S. Y. Yu and A. Kwasinski, "Technological assessment of dc-dc multiple-input converters as an interface for renewable energy applications," *Proceeding of the International Conference on Renewable Energy Research and Applications*, pp. 1-6, 2012.
- [5] A. Koran, T. Labella and L. J. Sheng, "High efficiency photovoltaic source simulator with fast response time for solar power conditioning systems evaluation," *IEEE Transactions on Power Electronics*, vol. 29, no. 3, pp. 1285-1297, 2014.
- [6] N. Mutoh, M. Ohno and T. Inoue, "A method for MPPT control while searching for parameters corresponding to weather conditions for PV generation systems," *IEEE Transactions on Industrial Electronics*, vol. 53, no. 4, pp. 1055-1065, 2008.
- [7] G. Petronea and C. A. Ramos-Pajab, "Modeling of photovoltaic fields in mismatched conditions for energy yield evaluations," *Electric Power Systems Research*, vol. 81, no. 4, pp. 1003-1013, 2011.
- [8] L. F. Lavado Villa, D. Picault, B. Raison, S. Bacha and A. Labonne, "Maximizing the power output of partially shaded photovoltaic plants through optimization of the interconnections among its modules," *IEEE Journal of Photovoltaics*, vol. 2, no. 2, pp. 154-163, 2012.
- [9] P.S. Rao, G. S. Ilango and C. Nagamani, "Maximum power from PV arrays using a fixed configuration under different shading conditions," *IEEE Journal of Photovoltaics*, vol. 4, no. 2, pp. 679-686, 2014.
- [10] L. Gao, R. A. Dougal, S. Liu and A. P. Iotova, "Parallel-connected solar PV system to address partial and rapidly fluctuating shadow conditions," *IEEE Transactions on Industrial Electronics*, vol. 56, no. 5, pp. 1548-1556, 2009.
- [11] R.A. Mastromauro, M. Liserre and A. D. Aquila, "Control issues in single-stage photovoltaic systems: MPPT, current, and voltage control," *IEEE Transactions on Industrial Informatics*, vol. 8, no. 2, pp. 241-254, 2012.
- [12] Y.J. Wang and P.C. Hsu, "Analytical modeling of partial shading and different orientation of photovoltaic modules," *IET Renewable Power Generation*, vol. 4, no. 3, pp. 272-282, 2010.
- [13] H. Patel and V. Agarwal, "Maximum power point tracking scheme for PV systems operating under partially shaded conditions," *IEEE Transactions on Industrial Electronics*, vol. 55, no. 4, pp. 1689-1698, 2008.
- [14] L. Zhang, W. G. Hurley and W. H. Wolfle, "A new approach to achieve maximum power point tracking for PV system with a variable inductor," *IEEE Transactions on Power Electronics*, vol. 26, no. 4,

- pp. 1031-1037, 2011.
- [15] R. F. Coelho, F. M. Concer and D. C. Martins, "A simplified analysis of dc-dc converters applied as maximum power point tracker in photovoltaic systems," *Proceedings of the IEEE International Symposium on Power Electronics for Distributed Generation Systems*, pp. 29-34, 2010.
- [16] D. W. Hart, "Power Electronics," McGraw-Hill Press, New York, pp. 196-265, 2011.
- [17] SANYO HIP 210-BO-1 Datasheet, 2010, Sanyo Electric Company, Ltd. Available: <http://www.solargy.com.sg/pdtsvc.php?subcat=HSP> VP&pid=HIP-210
- [18] W. H. Wolfle and W. G. Hurley, "Quasi-active power factor correction with a variable inductive filter: theory, design, and practice," *IEEE Transactions on Power Electronics*, vol. 18, no. 1, pp. 248-255, 2003.
- [19] T. Mori, K. Igarashi, K. Kanagawa, N. Yamashita, T. Shimizu and Y. Bizen, "Iron loss evaluation of iron powder core suitable for inductor used in power converters," *Proceeding of the International Conference on Power Electronics*, pp. 2983-2987, 2014.